ResearchGate

See discussions, stats, and author profiles for this publication at: https://www.researchgate.net/publication/6873538

Conformational Equilibrium in Alanine−Rich Peptides Probed by Reversible Stretching Simulations

ARTICLE *in* THE JOURNAL OF PHYSICAL CHEMISTRY B · SEPTEMBER 2006

Impact Factor: 3.3 · DOI: 10.1021/jp0601116 · Source: PubMed

CITATIONS
18

READS
17

3 AUTHORS, INCLUDING:

Jérôme Hénin
French National Centre for Scientific Research
28 PUBLICATIONS **1,097** CITATIONS
SEE PROFILE

Chris Chipot
French National Centre for Scientific Researc…
163 PUBLICATIONS **11,811** CITATIONS
SEE PROFILE

Available from: Chris Chipot
Retrieved on: 28 January 2016

Conformational Equilibrium in Alanine-Rich Peptides Probed by Reversible Stretching Simulations

Jérôme Hénin,[†] Klaus Schulten,[‡] and Christophe Chipot*[,†]

Équipe de Dynamique des Assemblages Membranaires, UMR CNRS/UHP No. 7565, Université Henri Poincaré, BP 239, 54506 Vandoeuvre-lès-Nancy Cedex, France, and Theoretical and Computational Biophysics Group, Beckman Institute, University of Illinois at Urbana−Champaign, Urbana, Illinois 61801

Received: January 6, 2006; In Final Form: May 14, 2006

Reversible stretching of the alanine-rich peptide 3K (*Proc. Natl. Acad. Sci. USA* **1989**, *86*, 5286−5290) and its analogue MW (*Nature* **1992**, *359*, 653−655) is examined using molecular dynamics simulations in explicit water. In both cases, sampling of the extension pathway is obtained on the 10 ns time scale by applying an adaptive biasing force. The free energy profile reveals a single minimum associated with a contiguous α-helix. Short 3_{10}-helical motifs are observed in folded as well as extended conformations, in accordance with their proposed role as folding intermediates. The native 3_{10}-helical content of both peptides is found, however, to be no higher than a few percent. Difficulties in both the definition and the detection of secondary structure motifs, most notably in relation to bifurcated hydrogen bonds, are proposed to account for the discrepancy between 3_{10}-helical propensities reported by several authors, based on experimental and computational results.

Introduction

Among elementary protein folding processes, formation of helical structures has prompted a number of investigations, both at the experimental and theoretical levels.[1] Although α-helices are significantly more frequent in known protein structures, 3_{10}-helices are also very common. They often occur as short segments, most of them consisting of less than two turns.[2] 3_{10}-helices have been proposed to act as intermediates in the folding pathway connecting the random coil to organized α-helices.[3] Hydrophobic peptides, particularly those with a high alanine content, are known for their propensity to form helical secondary structures in aqueous solution. Experimental contributions[4,5] have shown that alanine, of all naturally occurring amino acids, is the best helix stabilizer. The conformational inclination of alanine-rich peptides in aqueous solution toward helical motifs can be understood by the presence of titrable residues, e.g., lysine, that enhance solubilization and sequester at the same time water away from the backbone carbonyl and amino groups, hence promoting the formation of $i \rightarrow i + 4$ intramolecular hydrogen bonds.[6]

Millhauser suggested that 3_{10}-, rather than α-helices, may be the most favorable structure for many of such alanine-rich peptides.[7,8] On the other hand, Karle and Balaram put forward that preference toward α- over 3_{10}-helices increases with peptide length, and further argued that only peptides shorter than six residues are predominantly 3_{10}-helical.[9] The water-soluble, alanine-rich "3K" peptide designed by Baldwin and co-workers[10] has become a prototypical model for experimental and computational studies of the structure of helical protein segments. The 3K peptide, viz. Ac-$(AAAAK)_3$A-NH_2, contains three lysine residues conducive to water solubility and contributing to a large measure to helix stabilization.[6]

On the basis of circular dichroism (CD), Fourier transform infrared (FTIR), and spin-labeled electron spin resonance (ESR) spectra, Miick et al. proposed[7] that 3K predominantly adopts a 3_{10}-helical conformation in aqueous solution. This conclusion was later reinforced by proton NMR results[3,8] on the 3K peptide and its MW analogue, viz. Ac-AMAAK-AWAAK-AAAAR-A-NH_2. Yet, other experiments by Millhauser and co-workers on longer peptides[11] led to the conclusion that 3_{10}-helical preference decreases with peptide length, thereby concurring with the proposal of Karle and Balaram.[9]

Adaptation of Zimm−Bragg theory to multiple helical states by Sheinerman and Brooks[12] brought theoretical support to the views expressed by Millhauser. In a later, more quantitative study involving umbrella sampling simulations of helix propagation at the termini of polyalanine peptides of various lengths, Young and Brooks[13] concluded, however, that the 3_{10}-helix does not correspond to a local minimum of the corresponding free energy surfaces. Tirado-Rives et al.[14] had already reached this conclusion on the basis of their simulations of a polyalanine undecamer. On the basis of quantum mechanical calculations, Topol et al.[15] confirmed the α-helical preference of short alanine homopolymers and showed that the latter strongly depends on solvation effects. Noteworthily, in the light of their ESR investigation, Smythe et al. asserted that alanine-based peptides in aqueous solutions predominantly exist in an α-helix conformation,[16] and further put forth that the high population of 3_{10}-helices witnessed by Miick et al.[7] was artifactual and stemmed from the excessively flexible link connecting the spin label to the peptide backbone. Combining NMR and computational investigations of intrabackbone hydrogen-bonding patterns in 3K and the related Hlx peptide, Freedberg et al. observed predominant α-helical structures at the center of these peptides.[17]

A number of molecular simulations published in recent years have examined the helix−coil transition through extensive sampling of the conformational space, either by performing two-dimensional umbrella sampling[18,19] or replica-exchange molecular dynamics (MD)[20−25] simulations. An alternative route

* To whom correspondence should be addressed. E-mail: Christophe.Chipot@edam.uhp-nancy.fr.
† Équipe de Dynamique des Assemblages Membranaires.
‡ Theoretical and Computational Biophysics Group.

10.1021/jp0601116 CCC: $33.50 © 2006 American Chemical Society
Published on Web 08/01/2006

followed by Hiltpold et al. consists of reconstructing a two-dimensional free energy landscape from a number of long MD trajectories at different temperatures.[26] Earlier on, Smythe et al.[27] computed a free energy profile for the stretching of a helical α-aminobutyric acid (Aib)-based peptide toward an ensemble of extended forms in an implicit solvent.

The aim of the present contribution is to investigate the interconversion between helical and extended forms of the 3K and MW peptides, which is expected to allow putative 3_{10}-helical structures to be explored. To reach this goal, use was made of a recent methodology[28,29] targeted at the computation of free energy profiles based on an enhanced exploration of chosen conformational degrees of freedom. The adaptive biasing force (ABF) method uses a continuously updated estimate of a free energy profile to apply a bias that effectively erases energetic barriers as they are encountered, eventually leading to free diffusion of the system along the selected coordinate. The dynamics of the solvated 3K peptide was probed through a 22 ns unbiased MD simulation. In addition, each of the two peptides was investigated over 60 ns of equilibrium MD, employing the ABF scheme to sample the reversible unfolding process and compute the associated free energy profiles.

Computational Methods

The two peptides were solvated individually in a 45 × 45 × 45 Å^3 box containing 2919 TIP3P water molecules. Electric neutrality was obtained by adding one sodium and four chlorine ions, which altogether corresponds to an ionic strength of ca. 0.1 M. MD simulations were performed using the NAMD simulation package.[30] Isotropic periodic boundary conditions were applied. The unbiased simulation was run in the isobaric−isothermal ensemble at 300 K and 1 bar employing softly damped Langevin dynamics and the Langevin piston algorithm,[31] as implemented in NAMD.[32] Because volume fluctuations in such a system are marginal (assuming appropriate equilibration), trajectories for free energy calculations were generated in the canonical ensemble, starting from configurations equilibrated at 1 bar. The particle-mesh Ewald method was utilized to compute electrostatic interactions, and an 11 Å switched cutoff was applied to other nonbonded interactions. The *r*-RESPA multiple time-step integrator was used with a time step of 2 fs for short-range and 4 fs for long-range forces. Covalent bonds involving a hydrogen atom were constrained to their equilibrium length. All simulations reported here use the Cornell et al. AMBER95 force field,[33] which has been shown to describe appropriately the folding and the equilibrium structure of peptides.[34,35] Compared to the CHARMM27[36] force field available in NAMD, which exhibits a conspicuous tendency to overstabilize π-helical motifs in an unrealistic fashion,[37] AMBER95 behaves surprisingly well; albeit the shortcomings of this functional are equally well documented. Exaggeration of α-helicity in short peptides has been highlighted on the basis of sophisticated quantum mechanical calculations,[34] and a number of corrections of the force field have been put forth.[20,38,39] Yet, it is fair to state that, whereas these modifications correct some of the deficiencies of the original Cornell et al. force field, they also introduce new inaccuracies.[40] It is worth mentioning here the introduction of novel functionals[40,41] that are expected to improve the description of conformational equilibria in peptides. Probing these new force fields, which have not yet been widely utilized, falls clearly beyond the scope of the present work. Nevertheless, for comparison purposes, behavior of the 3K and MW peptides was probed using three different, well-established force fields, viz. AMBER95, OPLS-AA,[42] and CHARMM27. Finally, secondary structures were analyzed with the program STRIDE.[43]

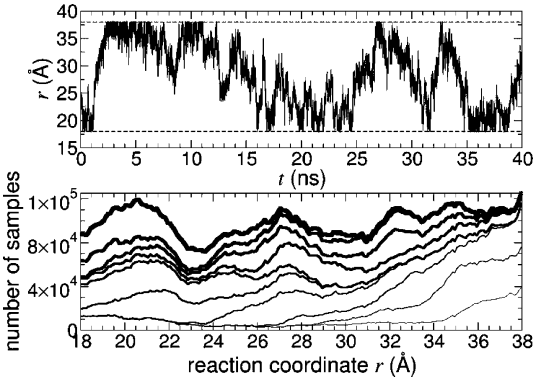

Figure 1. Top: Evolution of the reaction coordinate, *r*, as a function of time during the ABF simulation of the 3K peptide. Horizontal dashed lines indicate the limits of the sampling interval. Bottom: Sampling profile at different stages of the simulation. Thicker profiles reflect more sampling. The difference between two consecutive profiles represents 4 ns of sampling.

The free energy profiles delineating the transition from a fully folded, α-helical state to extended conformations were obtained by applying the ABF method of Darve and Pohorille[28] in its unconstrained formulation,[29] which does not require the computation of a constraint force. ABF enhances the reversible sampling of a pathway in conformational space by overcoming free energy barriers with a continuously refined bias while remaining in equilibrium conditions. Given a collective degree of freedom ξ, chosen as a putative reaction coordinate, ABF evaluates the free energy derivative with respect to ξ to estimate the appropriate biasing force on-the-fly. The free energy profile, or potential of mean force (PMF), is then recovered by thermodynamic integration along ξ. In the present case, the simple coordinate chosen to describe the unfolding of the 3K and MW peptides is the atom−atom distance, *r*, separating the first and the last carbonyl carbon atoms of the peptide chain. In the ABF simulations, *r* was confined to the interval spanning from 14 to 38 Å by means of harmonic restraining potentials. The unfolding simulation of each of the peptides was run for 60 ns. In the first 40 ns of the simulation of 3K, the smallest authorized value of *r* was 18 Å. At that point, it appeared that the free energy penalty for compressing the peptide to a length of 18 Å was rather small, and the lower bound of the interval was decreased to 14 Å for the rest of the simulation to sample a more repulsive part of the free energy landscape. An additional ABF simulation of the unfolding of 3K was performed using the gyration radius of the peptide as a generalized coordinate. The gyration radius was defined over all α-carbon atoms as the root-mean-square distance of these atoms to their center of mass.

Results and Discussion

Efficiency of the Sampling Strategy. Time evolution of the distance *r* during the first 40 ns of ABF simulation of the 3K peptide is shown in Figure 1. In the first 2.5 ns, the α-helix is progressively extended and disrupted as the energy barriers implied by the breaking of hydrogen bonds are sampled and overcome. The peptide then slowly folds back, and *r* begins to fluctuate freely, indicating that the computed profile effectively erases the free energy barriers experienced by the system.[28,29] In the remainder of the simulation, a number of accessible conformations are sampled for each value of *r*, thereby refining the PMF. The sampling history depicted in Figure 1 illustrates

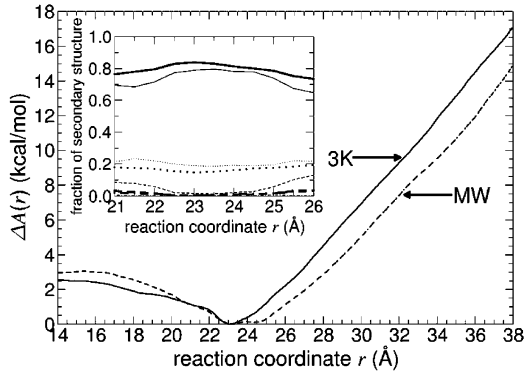

Figure 2. Free energy profile for the unfolding of the 3K (solid line) and the MW (dashed line) peptides. Inset: Probing nonergodicity effects by comparing the fractions of secondary structures inferred from simulations in the region of the free energy minimum, using a single, 24 Å wide interval (thick lines) and small, sequential windows (thin lines) viz. α-helix (solid lines), 3_{10}-helix (dashed lines), random coil (dotted lines), and turn (dotted−dashed lines).

how samples are accrued in successive strata covering the entire range of *r* with an increasing homogeneity as the simulation progresses. The simulation of MW behaved in a qualitatively similar way (data not shown).

The efficiency of the ABF sampling scheme in this case results from the appropriateness of the chosen generalized coordinate. Specifically, it is critical that this coordinate be a nonequivocal reduced description of the conformations accessible to the peptide. If a single value of *r* were associated with slowly interconverting conformations, the resulting PMF would poorly describe the energetics of the system, as has been shown for a simple peptide folding case.[44] Slow interconversion between states unresolved by an ill-chosen coordinate could not be accelerated efficiently by the adaptive bias, hence leading to hampered diffusion along *r*. The relevance of *r* as a reaction coordinate was investigated by computing a PMF for the unfolding of the 3K peptide, using its gyration radius as the chosen degree of freedom. Because there is no one-to-one correspondence between *r* and this parameter, quantitative comparison is not possible. The two profiles, however, appear to be in qualitative agreement. Moreover, the range of conformations sampled along the unfolding pathway does not depend on the choice of the coordinate, suggesting that the simulations presented here do not suffer from conformational biases, which could stem from nonequilibrium effects when using an ill-chosen generalized coordinate.

Closely related to the crucial choice of an appropriate generalized coordinate is the possibility of slowly relaxing, orthogonal degrees of freedom, prone to generate quasinonergodicity scenarios. In this event, relevant regions of the conformational space might be virtually never sampled. To ascertain that the present set of ABF free energy calculations circumvents this difficulty, an independent simulation of the 3K peptide has been performed in a restrained range of the reaction coordinate, *r*, around the native value, viz. $21 \leq r \leq 26$ Å. The starting point of this additional simulation corresponds to a semi-extended form of the peptide chain. The populations of the secondary structures were then compared to those obtained from the main trajectory spanning the entire reaction pathway. As may be seen in Figure2, the two sets of curves agree reasonably well, thereby suggesting that the behavior of the simulations is nearly ergodic. From this, it may be inferred that thermally accessible states are sampled exhaustively in the main trajectory.

Free Energy of the Unfolding Process. The free energy profile characterizing the 3K peptide in Figure *2* shows a single minimum at $r = 23.1$ Å, corresponding to the fully formed α-helix. A significant free energy penalty is required for visiting extended conformations, arising from the disruption of intramolecular hydrogen bonds responsible for the α-helix scaffold. In agreement with the shape of this PMF, the 22 ns unbiased simulation revealed only marginal fluctuations about the canonical α-helix. The chosen range of *r* does not allow compact, disordered conformations to be formed. The profile delineating the unfolding of the MW peptide only exhibits small differences with respect to that of 3K, with a similar shape and a single minimum located at $r = 23.2$ Å. The free energy penalties for extending or compressing the peptide are, however, slightly higher, which can be related to the larger helical propensity of MW.

Figure 3 shows a global secondary structure analysis of both peptides as a function of *r*, together with a breakdown on a per-residue basis. It reveals that, when both peptides are being extended, they gradually lose their essentially α-helical structure in favor of a mixture of turns, random coil, and to a limited extent, 3_{10}-helix. Comparing Figures 2 and 3, it is striking that the shape of the free energy profile is largely correlated to the α-helix content, presumably through the associated intramolecular hydrogen bonds.

Both MW and 3K appear to retain an appreciable fraction of α-helix content for any given value of *r,* albeit the percentile amount of α-helix is slightly larger for MW than 3K at large extensions. A plausible explanation for this general trend may be found in the amino acid sequence of the two peptides and the solvation properties of the constituent side chains. Of particular interest, closer inspection of the trajectories reveals that, in extended forms of either 3K or MW, the localized charged moiety of the titrable amino acids tends to remain perfectly hydrated. This result is in line with the contention of Vila et al.[6] that helix stabilization is promoted by charged residues, preserving the hydrogen-bond scaffold of the backbone from disruption by the surrounding water molecules.

Role of the 3_{10}-Helix. As has been concluded by Smythe et al.[27] for a short Aib-containing peptide, no local free energy minimum corresponds to a 3_{10}-helical conformation. Similarly, in the present contribution, Figure 3 shows that no particular value of *r* can be associated with a predominant 3_{10}-helical structure for either 3K or MW. A limited amount of 3_{10}-helix is, however, observed over the whole range of *r* values. Keeping this in mind, it becomes clear that the PMF cannot contain resolved energetic features characteristic of a 3_{10}-helix. In fact, a fully formed, contiguous 3_{10}-helix is never observed in the ABF simulation, albeit 3_{10}-helical segments as long as 11 residues are detected sporadically, over short time intervals. There are obviously energetic barriers for local transitions because of the necessary breaking and reforming of $i \rightarrow i + 3$ and $i \rightarrow i + 4$ intramolecular hydrogen bonds. Yet, these barriers are diluted in collective structural transitions involving a varying number of residues and occurring at any value of *r*.

Estimating the Native 3_{10}-Helix Content. Overall, the present ABF simulation highlights a very limited amount of 3_{10}-helical structure. The unbiased, equilibrium fraction of each secondary structure encountered can be estimated according to:

$$f_\alpha \propto \int_{r_{\min}}^{r_{\max}} \rho_\alpha(r) \exp[-\beta \Delta A(r)] r^2 \, dr$$

where f_α is the overall fraction of α-helical structure, $\rho_\alpha(r)$ is the fraction as a function of *r* as reported in Figure 3, and $\Delta A(r)$

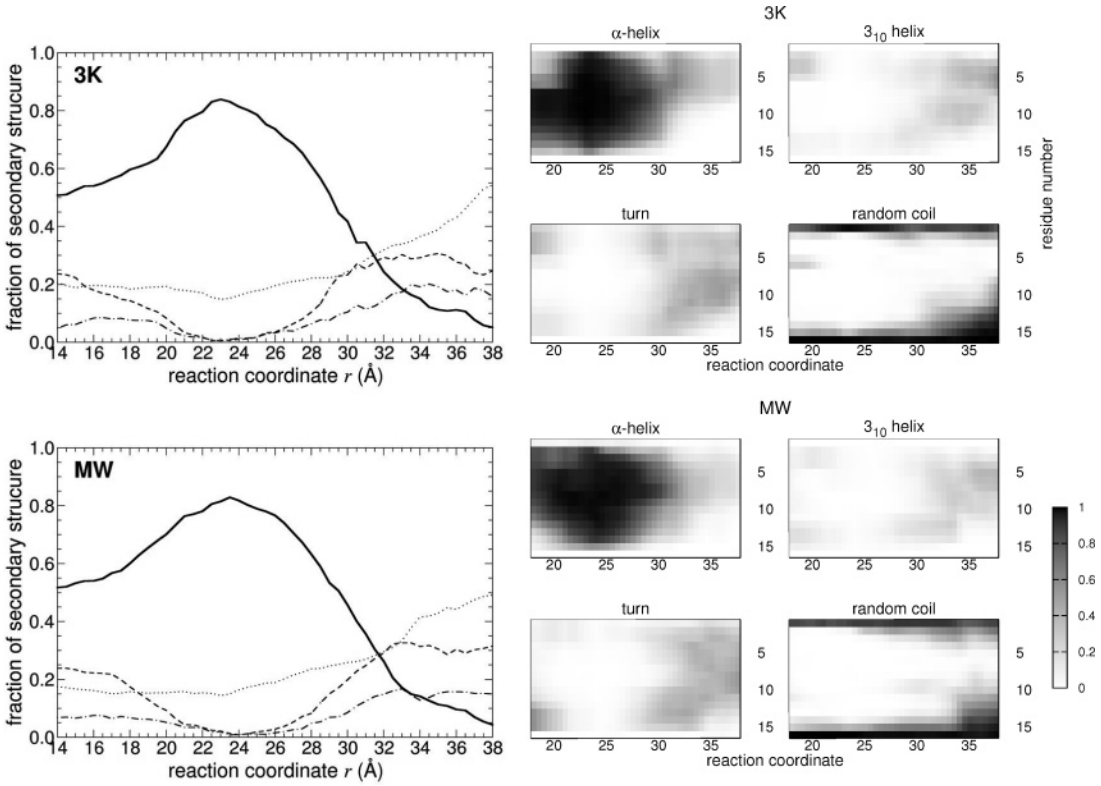

Figure 3. Secondary structure analysis as a function of the reaction coordinate, *r*, for the 3K (top) and the MW (bottom) peptides. Left: Overall decomposition in secondary structure elements as a function of *r*: α-helix (solid line), 3_{10}-helix (dashed line), random coil (dotted line), and turn (dotted−dashed line). Right: Fraction of each type of secondary structure as a function of *r* (abscissa) and the residue number (ordinate). The fraction of secondary structure is given by the color scale on the right-hand side.

TABLE 1: Theoretical Estimates of the Native Fractions of Secondary Structure in the 3K and the MW Peptides Determined from Multinanosecond MD Simulations

secondary structure element	α-helix, %	3_{10}-helix, %	turn, %	coil, %
3K peptide	79.5	1.8	2.4	16.3
MW peptide	79.6	1.8	2.5	16.1

is the free energy profile shown in Figure 2. $\beta^{-1} \equiv k_B T$, where k_B is the Boltzmann constant and T, the temperature. The predicted native fractions are given in Table 1. The secondary structure contents of the two peptides appear to be remarkably similar, justifying the use of MW as an analogue of 3K, designed to increase NMR signal dispersion.[8]

Quantitative results on the fraction of 3_{10}-helix found in alanine-rich peptides in aqueous solution are scarce. The interpretation of NMR spectra by Millhauser et al.[8] on MW suggests a high 3_{10}-helical propensity with a 50% probability at the termini and 25% in the middle of the peptide. These authors further note that MW is slightly less helical than 3K, which is not apparent from the results of the present comparative simulations. In line with previous observations,[9,11] Long and Tycko show[45] that preference toward α- over 3_{10}-helices increases with peptide length, and they argue that only peptides shorter than six residues are predominantly 3_{10}-helical, as would be the case in proteins.[46] They refer to the proposal of Millhauser et al. as "controversial", and they conclude that 3K is mostly α-helical. Yet, as was shown by Chipot and Pohorille in their folding simulation of the undecamer of polyleucine at the water−hexane interface,[47] a long-lived, contiguous 3_{10}-helix is witnessed on the pathway toward the α-helix, albeit in that case, conformation appears to be dictated to a large extent by the interfacial environment.

Armen et al.[48] find a strong contribution of π-helices and further propose that π-, rather than 3_{10}-helices, might play an essential role in helix−coil transitions. This viewpoint, however, has not been expressed in any other recent contribution to the literature. Furthermore, in some cases, occurrences of π-helices in peptide simulations have been regarded as force field artifacts,[17,37] which is confirmed by an unbiased simulation of the 3K peptide carried out here with the CHARMM27 force field. It is worth noting that the conspicuous tendency of this potential energy function to overstabilize π-helices has been corrected through a modification of backbone torsional potentials.[41] Following the trend witnessed with the AMBER force field, the additional unbiased simulation of 3K using OPLS-AA, starting from an ideal 3_{10}-helix, led to a rapid conversion of the peptide toward the α-helical conformation.

Whereas several experimental techniques have long provided an estimate of the total helical content of peptides, it seems that a quantitative analysis differentiating between α- and 3_{10}-helices is difficult to devise despite recent methodological advances. Experiments that give access to a measure of the 3_{10}-helix content[8] rely on a theoretical framework that involves stringent assumptions. Most of these techniques probe a few specific interatomic distances, thereby providing information on a local structure.[17] On the other hand, secondary structure assignment by computational tools such as STRIDE[43] might not be fully compatible with the conformational criteria utilized in experimental measurements. An analysis of hydrogen bonding in the peptide backbone using a simple distance criterion, viz. a 2.6 Å cutoff separating the carbonyl oxygen atom and the amino hydrogen atom, yields the bonding probabilities depicted in Figure 4. It can be deduced from the comparison of Figures 3 and 4 that, in many instances, $i \rightarrow i + 3$ bonded structures do

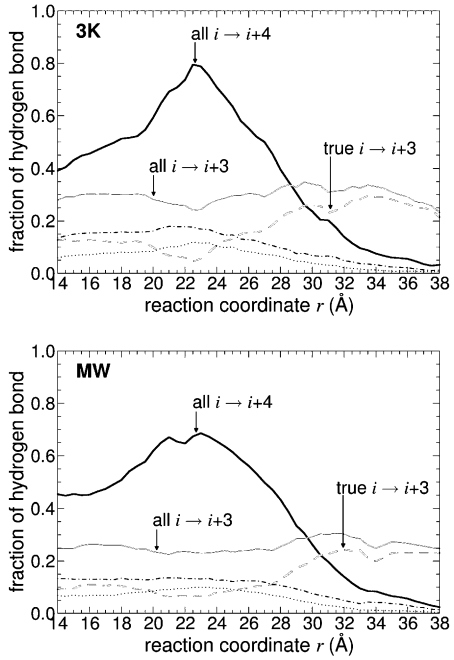

Figure 4. Fraction of hydrogen-bonding patterns in the 3K (top) and MW (bottom) peptides as a function of the reaction coordinate, r. The complete fraction of $i \rightarrow i + 4$ and $i \rightarrow i + 3$ intramolecular hydrogen bonds is represented by thick solid dark and light lines, respectively. True, nonbifurcated or double $i \rightarrow i + 3$ hydrogen bonds are shown as thick dashed light lines. Double, $N_{i+3}\cdots O_i\cdots N_{i+4}$, and bifurcated, $O_i\cdots N_{i+4}\cdots O_{i+1}$, hydrogen bonds are shown, respectively, as dark dotted−dashed and dotted lines.

not qualify as 3_{10}-helical under more rigorous criteria such as those implemented in STRIDE. Indeed, in these mostly α-helical structures, some intramolecular hydrogen bonds appear to be bifurcated $i \rightarrow i + 3$ and $i \rightarrow i + 4$ bonds, suggesting that the coupling constants measured in NMR experiments may be interpreted as a mixture of α- and 3_{10}-helices. Interestingly enough, this view is supported by experiment. From the ESR spectra of double-labeled alanine-rich peptides, Hanson et al.[49] conclude that α-helix is the predominant conformation. Yet, they observe α-helices consisting of 3.8 to 3.9 residues per turn, in lieu of the typical value of 3.6, thus suggesting a plastic structure that allows bifurcated hydrogen bonds to be formed. This nontrivial relationship between intramolecular hydrogen bonding and secondary structure appears to be no less crucial in the case of proteins, as was noted by Stickle et al.,[50] who suggested that the existence of multiply determined hydrogen bonds is likely to enhance the elasticity of an α-helix. A more recent statistical study on 1011 globular protein structures by Fain et al.[51] reveals that α-helices contain nearly as many $i \rightarrow i + 3$ bonds as $i \rightarrow i + 4$, the vast majority of them actually being either double, $N_{i+3}\cdots O_i\cdots N_{i+4}$, or bifurcated, $O_i\cdots N_{i+4}\cdots O_{i+1}$, bonds. Finally, the frequency of pure $i \rightarrow i + 3$ hydrogen bonds, i.e., neither bifurcated nor double, is closely related to the 3_{10}-helical content, as depicted in Figures 3 and 4.

Concluding Remarks

Association of the ABF method with a simple collective degree of freedom proves to constitute a well-adapted and efficient scheme for sampling the transition between helical and extended forms of short peptides in water. Describing systems of greater complexity with a number of correlated slow degrees of freedom would evidently require more sophisticated coordinates or multidimensional free energy landscapes.[18,19,52] The PMFs delineating the unfolding of the 3K and MW peptides exhibit a single free energy basin containing all compact, ordered structures, the minimum being an almost perfect α-helix, consistent with most experiments reported in the literature. 3_{10}-Helical motifs are observed, but only locally, and as transient structures. This supports the view that 3_{10}-helices act as the main intermediate conformation on the folding pathway toward the α-helical state.[3] The native secondary structures of the two peptides are found to be essentially identical, hence suggesting that MW is a relevant analogue of 3K for more discriminating NMR measurements.

Because of their minimalist nature, currently available empirical, macromolecular potential energy functions are not yet able to provide a fully reliable description of all proteins in every possible condition.[21,53,54] Ab initio quantum mechanical calculations are likely to become broadly applicable to short peptides in simplified solvent models,[15] thus partly bypassing the force field issue for those systems. The current evolution of modern force fields[40,55,56] requires very accurate experimental data, which may be available in the form of high-resolution structures of proteins, but paradoxically are harder to obtain for very dynamic objects such as soluble peptides. Quantitative experimental detection of 3_{10}- versus α-helices appears to be a daunting task. Additionally, classifying peptide conformations into prototypical secondary structures is rendered more difficult by the plastic nature of such conformations. We believe that experimental techniques capable of attaining that level of information are too recent for a clear consensus to be reached in the literature. Theoretical studies have suggested novel approaches,[57,58] the practical feasibility of which remains to be demonstrated.

Acknowledgment. We thank Dr. Andrew Pohorille, NASA Ames Research Center, for very helpful and stimulating discussions. The CRVHP project of LORIA, Nancy, France, is gratefully acknowledged for generous provision of the computer time used to conduct this research. K.S. acknowledges support from the National Institutes of Health (grant PHS 5 P41RR05969).

References and Notes

(1) Daggett, V. *Chem. Rev.* **2006**, *106*, 1898−1916.
(2) Barlow, D. J.; Thornton, J. M. *J. Mol. Biol.* **1988**, *201*, 601−619.
(3) Millhauser, G. L. *Biochemistry* **1995**, *34*, 3873−3877.
(4) O'Neil, K.; DeGrado, W. *Science* **1990**, *250*, 646−651.
(5) Chakrabartty, A.; Kortemme, T.; Baldwin, R. L. *Protein Sci*. **1994**, *3*, 843−852.
(6) Vila, J. A.; Ripoll, D. R.; Scheraga, H. A. *Biopolymers* **2001**, *58*, 235−246.
(7) Miick, S. M.; Martinez, G. V.; Fiori, W. R.; Todd, A. P.; Millhauser, G. L. *Nature* **1992**, *359*, 653−655.
(8) Millhauser, G. L.; Stenland, C. J.; Hanson, P.; Bolin, K. A.; van de Ven, F. J. *J. Mol. Biol.* **1997**, *267*, 963−974.
(9) Karle, I.; Balaram, P. *Biochemistry* **1990**, *29*, 6747−6756.
(10) Marqusee, S.; Robbins, V. H.; Baldwin, R. L. *Proc. Natl. Acad. Sci. U.S.A.* **1989**, *86*, 5286−5290.
(11) Fiori, W. R.; Miick, S. M.; Millhauser, G. L. *Biochemistry* **1993**, *32*, 11957−11962.
(12) Sheinerman, F. B.; Brooks, C. L., III. *J. Am. Chem. Soc.* **1995**, *117*, 10098−10103.
(13) Young, W. S.; Brooks, C. L. *J. Mol. Biol.* **1996**, *259*, 560−572.
(14) Tirado-Rives, J.; Maxwell, D. S.; Jorgensen, W. L. *J. Am. Chem. Soc.* **1993**, *115*, 11590−11593.
(15) Topol, I. A.; Burt, S. K.; Deretey, E.; Tang, T. H.; Perczel, A.; Rashin, A.; Csizmadia, I. G. *J. Am. Chem. Soc.* **2001**, *123*, 6054−6060.
(16) Smythe, M. L.; Nakaie, C. R.; Marshall, G. R. *J. Am. Chem. Soc.* **1995**, *117*, 10555−10562.
(17) Freedberg, D. I.; Venable, R. M.; Rossi, A.; Bull, T. E.; Pastor, R. W. *J. Am. Chem. Soc.* **2004**, *126*, 10478−10484.
(18) Samuelson, S. O.; Martyna, G. J. *J. Chem. Phys.* **1998**, *109*, 11061−11073.
(19) Samuelson, S. O.; Martyna, G. J. *J. Phys. Chem. B* **1999**, *103*, 1752−1766.

(20) García, A. E.; Sanbonmatsu, K. Y. *Proc. Natl. Acad. Sci. U.S.A.* **2002**, *99*, 2782−2787.
(21) Gnanakaran, S.; Nymeyer, H.; Portman, J.; Sanbonmatsu, K. Y.; García, A. E. *Cur. Opin. Struct. Biol.* **2003**, *13*, 168−174.
(22) Jas, G.; Kuczera, K. *Biophys. J.* **2004**, *87*, 3786−3798.
(23) Gnanakaran, S.; Hochstrasser, R. M.; García, A. E. *Proc. Natl. Acad. Sci. U.S.A.* **2004**, *101*, 9229−9234.
(24) Gnanakaran, S.; García, A. E. *Proteins* **2005**, *59*, 773−782.
(25) Paschek, D.; Gnanakaran, S.; García, A. E. *Proc. Natl. Acad. Sci. U.S.A.* **2005**, *102*, 6765−6770.
(26) Hiltpold, A.; Ferrara, P.; Gsponer, J.; Caflisch, A. *J. Phys. Chem. B* **2000**, *104*, 10080−10086.
(27) Smythe, M. L.; Huston, S. E.; Marshall, G. R. *J. Am. Chem. Soc.* **1995**, *117*, 5445−5452.
(28) Darve, E.; Pohorille, A. *J. Chem. Phys.* **2001**, *115*, 9169−9183.
(29) Hénin, J.; Chipot, C. *J. Chem. Phys.* **2004**, *121*, 2904−2914.
(30) Phillips, J. C.; Braun, R.; Wang, W.; Gumbart, J.; Tajkhorshid, E.; Villa, E.; Chipot, C.; Skeel, R. D.; Kalé, L.; Schulten, K. *J. Comput. Chem.* **2005**, *26*, 1781−1802.
(31) Feller, S. E.; Zhang, Y. H.; Pastor, R. W.; Brooks, B. R. *J. Chem. Phys.* **1995**, *103*, 4613−4621.
(32) Bhandarkar, M.; Brunner, R.; Chipot, C.; Dalke, A.; Dixit, S.; Grayson, P.; Gullingsrud, J.; Gursoy, A.; Hardy, D.; Hénin, J.; Humphrey, W.; Hurwitz, D.; Krawetz, N.; Kumar, S.; Nelson, M.; Phillips, J.; Shinozaki, A.; Zheng, G.; Zhu, F. *NAMD User's Guide*, version 2.6b1; Theoretical Biophysics Group, University of Illinois and Beckman Institute: Urbana, IL, 2005.
(33) Cornell, W. D.; Cieplak, P.; Bayly, C. I.; Gould, I. R.; Merz, K. M., Jr.; Ferguson, D. M.; Spellmeyer, D. C.; Fox, T.; Caldwell, J. C.; Kollman, P. A. *J. Am. Chem. Soc.* **1995**, *117*, 5179−5197.
(34) Beachy, M. D.; Chasman, D.; Murphy, R. B.; Halgren, T. A.; Friesner, R. A. *J. Am. Chem. Soc.* **1997**, *119*, 5908−5920.
(35) Duan, Y.; Kollman, P. A. *Science* **1998**, *282*, 740−744.
(36) MacKerell, A. D., Jr.; Bashford, D.; Bellott, M.; Dunbrack, R. L., Jr.; Evanseck, J. D.; Field, M. J.; Fischer, S.; Gao, J.; Guo, H.; Ha, S.; Joseph-McCarthy, D.; Kuchnir, L.; Kuczera, K.; Lau, F. T. K.; Mattos, C.; Michnick, S.; Ngo, T.; Nguyen, D. T.; Prodhom, B.; Reiher, W. E., III; Roux, B.; Schlenkrich, M.; Smith, J. C.; Stote, R.; Straub, J.; Watanabe, M.; Wiórkiewicz-Kuczera, J.; Yin, D.; Karplus, M. *J. Phys. Chem. B* **1998**, *102*, 3586−3616.
(37) Feig, M.; MacKerell, A. D.; Brooks, C. L., III. *J. Phys. Chem. B* **2003**, *107*, 2831−2836.
(38) Kollman, P.; Dixon, R.; Cornell, W.; Fox, T.; Chipot, C.; Pohorille, A. In *Computer Simulation of Biomolecular Systems: Theoretical and Experimental Applications*; Van Gunsteren, W. F., Weiner, P. K., Eds.; Escom: Leiden, The Netherlands, 1997; pp 83−96.
(39) Wang, J.; Cieplak, P.; Kollman, K. P. *J. Comput. Chem.* **2000**, *21*, 1049−1074.
(40) Sorin, E. J.; Pande, V. S. *Biophys. J.* **2005**, *88*, 2472−2493.
(41) MacKerell, A. D.; Feig, M.; Brooks, C. L. *J. Am. Chem. Soc.* **2004**, *126*, 698−699.
(42) Kaminski, G. A.; Friesner, R. A.; Tirado-Rives, J.; Jorgensen, W. L. *J. Phys. Chem. B* **2001**, *105*, 6474−6487.
(43) Frishman, D.; Argos, P. *Proteins* **1995**, *23*, 566−579.
(44) Chipot, C.; Hénin, J. *J. Chem. Phys.* **2005**, *123*, 244906.
(45) Long, H.; Tycko, R. *J. Am. Chem. Soc.* **1998**, *120*, 7039−7048.
(46) Pal, L.; Chakrabarti, P.; Basu, G. *J. Mol. Biol.* **2003**, *326*, 273−291.
(47) Chipot, C.; Pohorille, A. *J. Am. Chem. Soc.* **1998**, *120*, 11912−11924.
(48) Armen, R.; Alonso, D. O. V.; Daggett, V. *Protein Sci.* **2003**, *12*, 1145−1157.
(49) Hanson, P.; Anderson, D.; Martinez, G.; Millhauser, G.; Formaggio, F.; Crisma, M.; Toniolo, C.; Vita, C. *Mol. Phys.* **1998**, *95*, 957−966.
(50) Stickle, D. F.; Presta, L. G.; Dill, K. A.; Rose, G. D. *J. Mol. Biol.* **1992**, *226*, 1143−1159.
(51) Fain, A. V.; Berezovsky, I. N.; Chekhov, V. O.; Ukrainskii, D. L.; Esipova, N. G. *Biophysics* **2001**, *46*, 921−928.
(52) Guo, Z.; Brooks, C. L.; Boczko, E. M. *Proc. Natl. Acad. Sci. U.S.A.* **1997**, *94*, 10161−6.
(53) Yoda, T.; Sugita, Y.; Okamoto, Y. *Chem. Phys.* **2004**, *307*, 269−283.
(54) Yoda, T.; Sugita, Y.; Okamoto, Y. *Chem. Phys. Lett.* **2004**, *386*, 460−467.
(55) Price, D. J.; Brooks, C. L., III *J. Comput. Chem.* **2002**, *23*, 1045−1057.
(56) Sorin, E. J.; Pande, V. S. *J. Comput. Chem.* **2005**, *26*, 682−90.
(57) Moran, A. M.; Park, S.-M.; Dreyer, J.; Mukamel, S. *J. Chem. Phys.* **2003**, *118*, 3651−3659.
(58) Kim, S.; Cross, T. A. *J. Magn. Reson.* **2004**, *168*, 187−193.